Published online 20 August 2008 *Nucleic Acids Research, 2008, Vol. 36, No. 17* ***5441–5450***
doi:10.1093/nar/gkn516

Biochemical analysis of the N-terminal domain of human RAD54B

Naoyuki Sarai[1,2], Wataru Kagawa[1], Norie Fujikawa[1], Kengo Saito[1,3], Juri Hikiba[3], Kozo Tanaka[4], Kiyoshi Miyagawa[5], Hitoshi Kurumizaka[1,3,*] and Shigeyuki Yokoyama[1,2]

[1]Systems and Structural Biology Center, Yokohama Institute, RIKEN, 1-7-22 Suehiro-cho, Tsurumi, Yokohama 230-0045, [2]Department of Biophysics and Biochemistry, Graduate School of Science, The University of Tokyo, 7-3-1 Hongo, Bunkyo-ku, Tokyo 113-0033, [3]Graduate School of Advanced Science and Engineering, Waseda University, 2-2 Wakamatsu-cho, Shinjuku-ku, Tokyo 162-8480, [4]Institute of Development, Aging and Cancer, Tohoku University, 4-1 Seiryo-machi, Aoba-ku, Sendai 980-8575 and [5]Laboratory of Molecular Radiology, Center of Disease Biology and Integrative Medicine, Graduate School of Medicine, The University of Tokyo, 7-3-1 Hongo, Bunkyo-ku, Tokyo 113-0033, Japan

Received April 25, 2008; Revised July 16, 2008; Accepted July 29, 2008

ABSTRACT

The human RAD54B protein is a paralog of the RAD54 protein, which plays important roles in homologous recombination. RAD54B contains an N-terminal region outside the SWI2/SNF2 domain that shares less conservation with the corresponding region in RAD54. The biochemical roles of this region of RAD54B are not known, although the corresponding region in RAD54 is known to physically interact with RAD51. In the present study, we have biochemically characterized an N-terminal fragment of RAD54B, consisting of amino acid residues 26–225 (RAD54B$_{26–225}$). This fragment formed a stable dimer in solution and bound to branched DNA structures. RAD54B$_{26–225}$ also interacted with DMC1 in both the presence and absence of DNA. Ten DMC1 segments spanning the entire region of the DMC1 sequence were prepared, and two segments, containing amino acid residues 153–214 and 296–340, were found to directly bind to the N-terminal domain of RAD54B. A structural alignment of DMC1 with the *Methanococcus voltae* RadA protein, a homolog of DMC1 in the helical filament form, indicated that these RAD54B-binding sites are located near the ATP-binding site at the monomer–monomer interface in the DMC1 helical filament. Thus, RAD54B binding may affect the quaternary structure of DMC1. These observations suggest that the N-terminal domain of RAD54B plays multiple roles of in homologous recombination.

INTRODUCTION

Homologous recombination is involved in many biologically important processes, and it occurs in all organisms (1–3). In meiosis, homologous recombination is carried out in order to generate genetic diversity, by creating new linkage arrangements between genes or parts of genes. Meiotic recombination also contributes to the establishment of a physical connection between homologous chromosomes, which is essential for proper chromosome segregation (4,5).

Meiotic recombination is initiated by a programed double-strand break (DSB) introduced in the initiation sites for recombination (6). At the DSB site, a single-stranded DNA (ssDNA) tail is produced, and it is incorporated into a protein–DNA complex, called the presynaptic filament. This presynaptic filament catalyzes the homologous pairing and strand-exchange reactions. An intermediate structure, called the Holliday junction, in which two double-stranded DNA (dsDNA) molecules form a four-way junction, is generated through the homologous-pairing and strand-exchange steps. The Holliday junction is then resolved into two DNA molecules by the action of endonucleases.

Studies in the budding yeast *Saccharomyces cerevisiae* initially identified the *rad52* epistasis group of genes (*rad50*, *rad51*, *rad52*, *rad54*, *rdh54*/*tid1*, *rad55*, *rad57*, *rad59*, *mre11* and *xrs2*) as the core factors of the homologous recombination machinery. The functions of the *rad52* epistasis group genes are highly conserved among eukaryotes, from yeast to human (7,8). One member of this group of genes, *rad54*, encodes a protein that belongs to the SWI2/SNF2 protein family, whose members have

*To whom correspondence should be addressed. Tel: +81 3 5369 7315; Fax: +81 3 5367 2820; Email: kurumizaka@waseda.jp
Correspondence may also be addressed to Shigeyuki Yokoyama. Tel: +81 3 5841 4395; Fax: +81 3 5841 8057;
Email: yokoyama@biochem.s.u-tokyo.ac.jp

DNA-dependent ATPase and chromatin-remodeling activities (9–15). Recent studies suggested that Rad54 may play diverse roles in multiple stages of homologous recombination (16,17). Rad54 promotes and stabilizes the Rad51–ssDNA nucleoprotein filament formation by physically interacting with Rad51 (18–21), and it also stimulates the homologous pairing and strand-exchange reactions mediated by Rad51 (22–25). These facts suggest that Rad54 functions in the early stage of homologous recombination. Rad54 is also known to disassemble Rad51 nucleoprotein filaments from DNA, which may be essential in the later stages of recombination (26). Moreover, Rad54 promotes branch migration of the Holliday junction in an ATP-dependent manner, suggesting that Rad54 functions in the late stage of recombination (25).

RAD54B, which shares homology with Rad54, was identified in the human cell as a member of the SWI2/SNF2 family proteins (27). Like Rad54, RAD54B is a DNA-dependent ATPase and stimulates the RAD51-mediated homologous pairing (28,29). Previously, our group and others reported that RAD54B stimulates the recombination activity of DMC1, a meiosis-specific RAD51 homolog, suggesting its role in meiotic homologous recombination (30–32). Therefore, Rad54B may be a paralog of Rad54 having both overlapping and non-overlapping roles with those of Rad54. RAD54B contains helicase motifs, which are commonly found in the members of the SWI2/SNF2 family. Outside this region, RAD54B has an N-terminal region of ~300 amino acid residues. The corresponding region in RAD54 directly interacts with RAD51 (19), suggesting that the N-terminal region of RAD54B may also be essential for the interactions with other recombination factors. However, the N-terminal region of RAD54B is considerably longer than that of RAD54. Hence, it is of interest whether the N-terminal region of RAD54B contains functional regions that are not present in that of RAD54. In the present study, we identified a stable N-terminal domain of the human RAD54B protein, and found that this domain is capable of self-associating, binding to DNA and interacting with both RAD51 and DMC1. These observations suggest multifunctional roles of the N-terminal domain of RAD54B in homologous recombination.

MATERIALS AND METHODS

Purification of RAD54B$_{26–225}$

The His$_6$-tagged human RAD54B$_{26–225}$ protein was overexpressed in the *Escherichia coli* JM109 (DE3) strain carrying an expression vector for the minor tRNAs [Codon(+)RIL, (Novagen, Darmstadt, Germany)], using the pET15b expression system (Novagen). Harvested cells were disrupted by sonication in buffer A (pH 7.8), containing 50 mM Tris–HCl, 0.3 M KCl, 2 mM 2ME, 10% glycerol and 5 mM imidazole. Lysates were mixed gently by the batch method with 4 ml Ni-NTA beads at 4°C for 1 h. The RAD54B$_{26–225}$-coupled Ni-NTA agarose beads were then packed into an Econo-column (Bio-Rad Laboratories, Hercules, CA, USA) and were washed with 30 CV of buffer B (pH 7.8), which contained 50 mM Tris–HCl, 0.3 M KCl, 2 mM 2ME, 10% glycerol and 20 mM imidazole. The His$_6$-tagged RAD54B$_{26–225}$ was eluted in a 30 CV linear gradient of 20–300 mM imidazole in buffer B. RAD54B$_{26–225}$, which eluted in a broad peak, was collected and treated with 2 U of thrombin protease (GE Healthcare, Biosciences, Uppsala, Sweden) per milligram of RAD54B$_{26–225}$. The RAD54B$_{26–225}$ protein was then dialyzed against buffer C (pH 7.2), which contained 20 mM HEPES–KOH, 0.1 M KCl, 0.5 mM EDTA, 2 mM 2ME and 10% glycerol, and was mixed with 2 ml of Benzamidine-Sepharose (GE Healthcare) column matrix at 4°C for 1 h. The proteins in the Benzamidine-Sepharose flow-through fraction were mixed with 8 ml of Q-Sepharose column matrix at 4°C for 1 h. The proteins in the Q-Sepharose flow-through fraction were then mixed with 8 ml of SP-Sepharose column matrix at 4°C for 1 h. The SP-Sepharose column was washed with 20 CV of buffer C, and the RAD54B$_{26–225}$ protein was eluted with a 20 CV linear gradient from 0.1 to 1.0 M KCl in this buffer. The peak fractions of the RAD54B$_{26–225}$ proteins were collected, dialyzed against buffer D (pH 7.5), which contained 20 mM HEPES–KOH, 0.1 M KCl, 0.5 mM EDTA, 2 mM 2ME and 10% glycerol, and stored at –80°C.

Purification of the DMC1 deletion mutants

Ten overlapping glutathione *S*-transferase (GST)-fused DMC1 deletion mutants, composed of amino acid residues 1–44, 24–66, 47–104, 84–126, 118–162, 153–214, 195–237, 225–270, 264–306 and 296–340, respectively, were overexpressed in the *E. coli* JM109 (DE3) strain carrying an expression vector for the minor tRNAs [Codon(+)RIL], using the pET41b expression system (Novagen). The cells were suspended in buffer E (pH 8.0), containing 50 mM Tris–HCl, 0.3 M KCl, 2 mM 2ME, 5 mM EDTA and 10% glycerol, and were disrupted by sonication. Lysates were mixed gently by the batch method with 500 µl Glutathione Sepharose 4B (GS4B) beads (GE Healthcare) at 4°C for 1 h. The beads bound with the GST–DMC1 deletion mutants were then washed four times with 10 ml of buffer E. The GST–DMC1 deletion mutants were eluted by 1 ml of buffer E with 20 mM glutathione. These proteins were dialyzed against buffer E and were stored at 4°C.

The RAD51 and DMC1 proteins were purified as described previously (30,33,34). The concentrations of the purified proteins were determined with a Bio-Rad protein assay kit, using BSA as the standard.

DNA substrates

The ϕX174 circular ssDNA and replicative form I DNA were purchased from New England Biolabs, Ipswich, MA, USA and Life Technologies, Gaithersburg, MD, USA. The concentrations of these DNA are expressed as molar nucleotide concentrations. The oligonucleotides used in this study are shown in Table 1. They were purchased from Invitrogen, Carlsbad, CA, USA, in the desalted form, and were purified by anion exchange

Table 1. Oligonucleotides used in this study

Name	Length	Sequence (5′ to 3′)
PolyA	44-mer	AAAAAAAAAAAAAAAAAAAAAAAAAAAAAAAAAAAAAAAAAAAA
2	50-mer	TGGGTCAACGTGGGCAAAGATGTCCTAGCAATGTAATCGTCTATGACGTT
2a	50-mer	AACGTCATAGACGATTACATTGCTAGGACATCTTTGCCCACGTTGACCCA
5	50-mer	TGCCGAATTCTACCAGTGCCAGTGATGGACATCTTTGCCCACGTTGACCC
6	50-mer	GTCGGATCCTCTAGACAGCTCCATGATCACTGGCACTGGTAGAATTCGGC
7	50-mer	CAACGTCATAGACGATTACATTGCTACATGGAGCTGTCTAGAGGATCCGA
8	51-mer	CAACGTCATAGACGATTACATTGCTAATCACTGGCACTGGTAGAATTCGGC
10	24-mer	GGACATCTTTGCCCACGTTGACCC
15	26-mer	TGCCGAATTCTACCAGTGCCAGTGAT

chromatography. Briefly, the oligonucleotides were dissolved in water and applied to a MonoQ column (GE Healthcare) equilibrated with 10 mM NaOH. Oligonucleotides 2, 2a, 5, 6, 7 and 8 were eluted in a two-step linear gradient, consisting of 5 column volumes of 0–0.6 M NaCl followed by 50 column volumes of 0.6–0.9 M NaCl. Oligonucleotides 10 and 15 were also eluted in a two-step linear gradient, consisting of 5 column volumes of 0–0.5 M NaCl followed by 50 column volumes of 0.5–0.8 M NaCl. Peak fractions were collected, ethanol precipitated and dissolved in water. The substrates with various structures were made by annealing appropriate combinations of oligonucleotides, as described previously (35–37). The combinations of oligonucleotides were as follows: dsDNA, oligonucleotides 2 and 2a; Splayed arm, oligonucleotides 2 and 8; 3′-tailed duplex, oligonucleotides 2 and 10; 5′-tailed duplex, oligonucleotides 8 and 15; 3′-flapped DNA, oligonucleotides 2, 8 and 10; 5′-flapped DNA, oligonucleotides 2, 8 and 15; 3′-PX junction, oligonucleotides 2, 6, 7 and 10; 5′-PX junction, oligonucleotides 2, 6, 7 and 15; and X junction, oligonucleotides 2, 5–7. Oligonucleotide substrates are expressed as molar molecule concentrations.

Gel filtration analysis of $RAD54B_{26–225}$

$RAD54B_{26–225}$ was concentrated to 5.6 mg/ml and 50 µl of the concentrated protein was fractionated through a 25 ml Superdex 200 10/30 GL column (GE Healthcare) using buffer G.

DNA-binding assays of $RAD54B_{26–225}$

For the plasmid DNA-binding assay, the indicated amounts of $RAD54B_{26–225}$ were incubated with ϕX174 ssDNA (20 µM) or ϕX174 dsDNA (10 µM) at 37°C for 20 min in 10 µl of buffer H, containing 50 mM Tris–HCl (pH 7.8), 100 µg/ml BSA and 1mM DTT. After 10-fold loading dye was added, the products were resolved by 1% agarose gel electrophoresis in TAE buffer at 3.3 V/cm for 2.5 h, and were visualized by staining with ethidium bromide. For the binding assays using oligonucleotide substrates, the indicated amounts of $RAD54B_{26–225}$ were incubated with the DNA substrates (0.2 µM) at 37°C in 10 µl of buffer H for either 10 min for ssDNA or 20 min for other substrates. $A^{32}P$-labeled polyA oligonucleotide was used as the ssDNA substrate, and the resulting $RAD54B_{26–225}$–polyA complex was resolved by 1% agarose gel electrophoresis in 0.5 × TBE buffer at 3.3 V/cm for 2 h. The gel was dried, exposed to an imaging plate and visualized using a BAS2500 image analyzer (Fuji Film Co., Tokyo, Japan). For other DNA substrates containing various structures, the complexes with $RAD54B_{26–225}$ were resolved by 5% polyacrylamide gel electrophoresis in 1 × TBE buffer at 100 V for 50 min, and were visualized by staining with ethidium bromide.

Protein–protein binding assay of $RAD54B_{26–225}$

$RAD54B_{26–225}$ was covalently conjugated to Affi-Gel 15 beads (100 µl, Bio-Rad), according to the manufacturer's instructions. The unbound proteins were removed by washing the beads five times with binding buffer F (pH 7.5), which contained 20 mM HEPES–KOH, 0.15 M KCl, 0.5 mM EDTA, 2 mM 2ME, 10% glycerol and 0.05% Triton X-100. To block the residual active ester sites, ethanolamine (pH 8.0) was added to a final concentration of 100 mM and the resin was incubated at 4°C overnight. After washing the resin five times with 500 µl of buffer F, the Affi-Gel 15-protein matrices were adjusted to 50% slurries with buffer F and were stored at 4°C. For the binding assay, 20 µl of the Affi-Gel 15-protein slurry were mixed with 20 µg of RAD51, DMC1 or RecA at room temperature for 2 h. The Affi-Gel 15-protein beads were then washed five times with 500 µl of buffer F. SDS–PAGE sample buffer (2-fold) was mixed directly with the washed beads. After heating the mixture at 98°C for 5 min, the proteins were fractionated by 12% SDS–PAGE. Bands were visualized by Coomassie Brilliant Blue staining.

In the GS4B pull-down assay, GS4B beads (30 µl) were equilibrated with buffer G, containing 20 mM Tris–HCl (pH 8.0), 0.2 M KCl, 2 mM 2ME, 5 mM EDTA, 10% glycerol and 0.1% NP-40, and were mixed with 10 µg of the GST–DMC1 deletion mutants at 4°C for 30 min. To prevent nonspecific interactions between $RAD54B_{26–225}$ and the GS4B beads, the GS4B–DMC1 deletion mutants were first incubated with 500 µg/ml BSA, and the reaction was incubated at 4°C for 30 min, followed by the addition of 10 µg of $RAD54B_{26–225}$. After an incubation at 4°C for 1 h, the GS4Bbeads were washed with buffer G five times and were eluted with SDS–PAGE sample buffer.

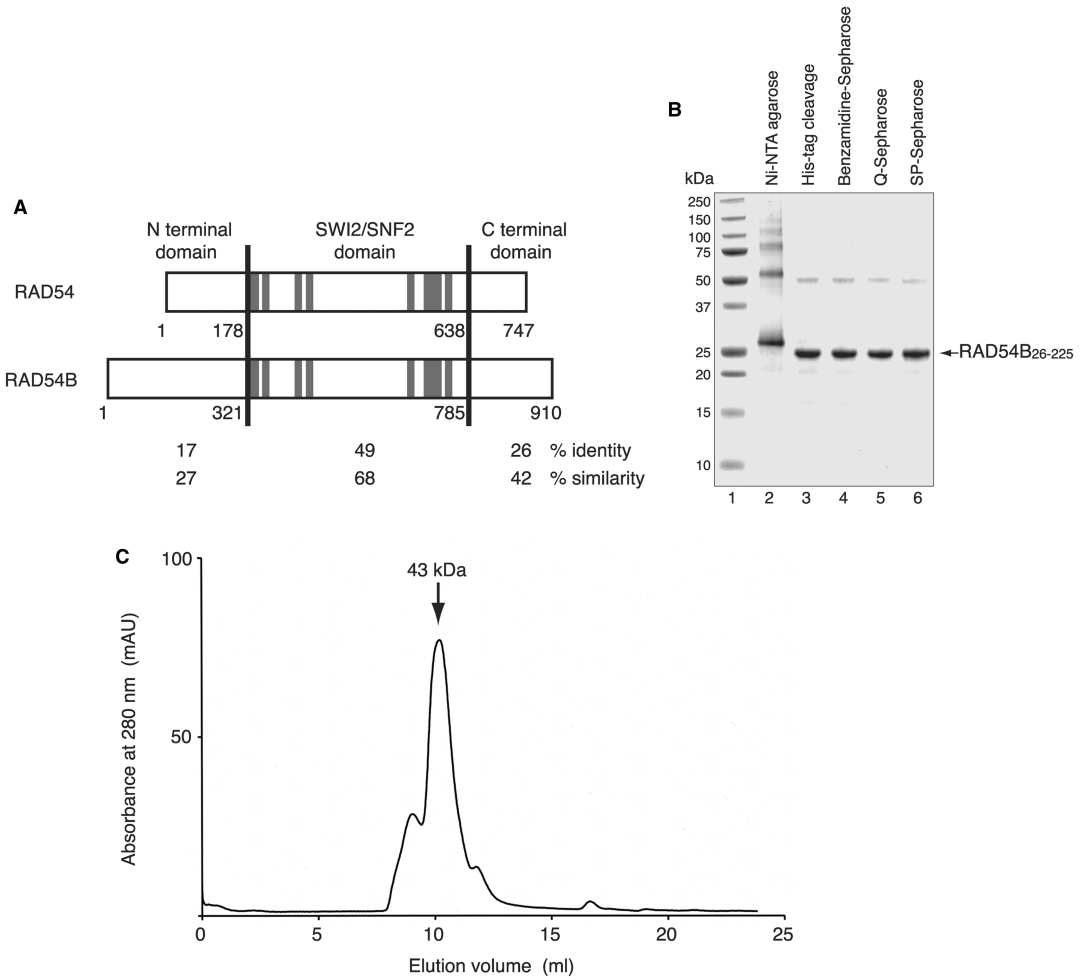

Figure 1. (**A**) Sequence comparison of RAD54 and RAD54B. These proteins are separated into three regions (N-terminal domain, SWI2/SNF2 domain and C-terminal domain), and the amino acid sequence identities and similarities between these proteins were calculated for each region. The amino acid number at the boundary of each domain is denoted. The gray lines indicate the seven helicase motifs (I, Ia, II, III, IV, V and VI, respectively). (**B**) Purification of the $RAD54B_{26–225}$ protein. The peak fractions from the Ni-NTA agarose column (lane 2), the fraction after the removal of the His_6 tag (lane 3), the Benzamidine Sepharose flow-through (lane 4), the Q-Sepharose flow-through (lane 5) and the peak fractions from the SP-Sepharose column (lane 6) were analyzed on a 12% SDS–PAGE gel, which was stained with Coomassie Brilliant Blue. Lane 1 indicates the molecular mass markers. (**C**) Gel filtration analysis of $RAD54B_{26–225}$. The arrow indicates the peak location of a molecular weight marker, ovalbumin (43 kDa), which nearly corresponds to that of $RAD54B_{26–225}$.

ssDNA- and dsDNA-binding assays of DMC1

The indicated amounts of DMC1 were incubated with ϕX174 ssDNA (20 μM) or ϕX174 dsDNA (10 μM) at 37°C for 20 min in 10 μl of buffer I, containing 50 mM Tris–HCl (pH 7.8), 1 mM ATP, 2 mM $MgCl_2$, 100 μg/ml BSA and 1 mM DTT. After 10-fold loading dye was added, the products were resolved by 1% agarose gel electrophoresis in TAE buffer at 3.3 V/cm for 2.5 h, and were visualized by staining with ethidium bromide.

Interaction between DMC1 and $RAD54B_{26–225}$ on ssDNA and dsDNA

The reactions were started by incubating 40 μM DMC1 with 20 μM ϕX174 ssDNA or 10 μM ϕX174 dsDNA at 37°C for 20 min, in 10 μl of buffer I. The indicated amounts of $RAD54B_{26–225}$ were then incorporated, and the mixtures were incubated at 37°C for 20 min. After 10-fold loading dye was added, the products were resolved by 1% agarose gel electrophoresis in TAE buffer at 3.3 V/cm for 2.5 h. To determine whether DMC1 was present, the protein–DNA complex was localized by ethidium bromide staining of the agarose gel, and the corresponding area of the gel was excised for electroelution. The eluted proteins were fractionated by 12% SDS–PAGE, and the bands were visualized by Coomassie Brilliant Blue staining.

RESULTS

Purification of the RAD54B N-terminal domain fragment

To gain insight into the function of the N-terminal region of RAD54B, which is less conserved between RAD54 and RAD54B (Figure 1A), we constructed a RAD54B deletion mutant containing the first 295 residues ($RAD54B_{1–295}$).

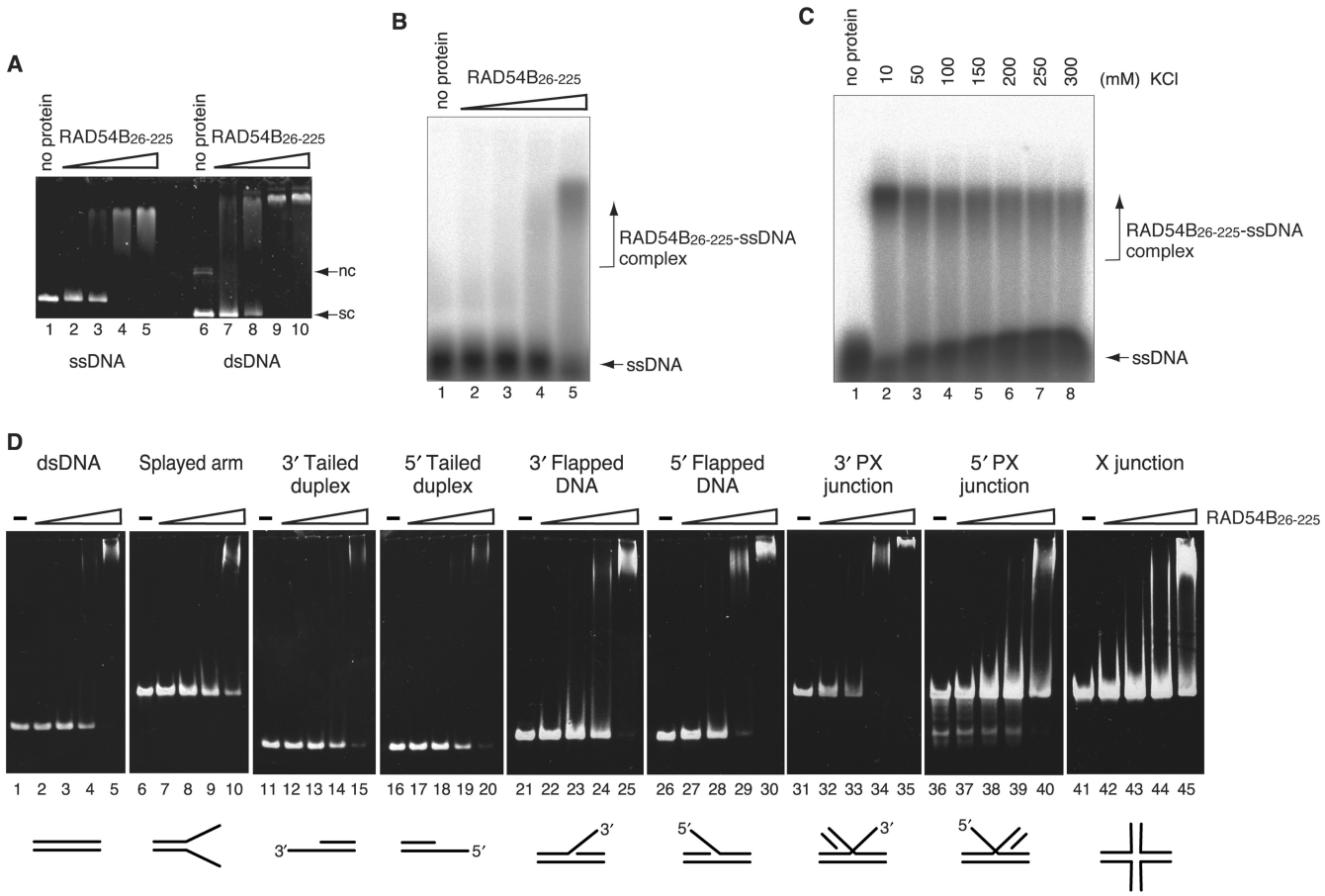

Figure 2. DNA-binding activity of $RAD54B_{26–225}$. (**A**) Plasmid ssDNA (20 μM in nucleotides, lanes 1–5) or plasmid superhelical dsDNA (10 μM in nucleotides, lanes 6–10) was incubated with $RAD54B_{26–225}$ at 37°C for 20 min. The concentrations of $Rad54B_{26–225}$ used in the DNA-binding experiments were 2.0 μM (lanes 2 and 7), 4.0 μM (lanes 3 and 8), 8.0 μM (lanes 4 and 9) and 16 μM (lanes 5 and 10). The reaction mixtures were fractionated on a 1% agarose gel, which was stained with ethidium bromide. Nc and sc indicate nicked circular and superhelical dsDNA, respectively. (**B**) A ^{32}P labeled single-stranded oligonucleotide (polyA 44-mer, 0.2 μM in molecules) was incubated with $RAD54B_{26–225}$ (2, 4, 8 or 16 μM) at 37°C for 10 min and the reaction mixtures were fractionated on a 1% agarose gel. (**C**) Salt concentration titration for the $RAD54B_{26–225}$–polyA complex. $RAD54B_{26–225}$ (16 μM) was incubated with a ^{32}P labeled single-stranded oligonucleotide (polyA 44-mer, 0.2 μM in molecules) in the reaction mixture containing the indicated concentrations of KCl. The reaction mixtures were fractionated on a 1% agarose gel. (**D**) Various branched DNA substrates (0.2 μM in molecules) were incubated with $RAD54B_{26–225}$ (2, 4, 8 or 16 μM) at 37°C for 20 min, and the reaction mixtures were fractionated on a 5% polyacrylamide gel, which was stained with ethidium bromide.

However, this fragment rapidly degraded to several smaller fragments during the expression and purification processes, suggesting that the fragment contained unstructured or flexible regions. Several rounds of fragment design and purification were performed to identify the stable N-terminal region of RAD54B. We found that the fragment consisting of amino acid residues 26–225 of RAD54B ($RAD54B_{26–225}$) was resistant to proteolysis and was highly soluble. The $RAD54B_{26–225}$ mutant was expressed in the *E. coli* JM109 (DE3) strain, as a fusion protein with an N-terminal His_6 tag containing a cleavage site for thrombin protease, and was purified by Ni-NTA column chromatography (Figure 1B, lane 2). After the His_6 tag was uncoupled with thrombin protease (Figure 1B, lane 3), the peak fractions containing $RAD54B_{26–225}$ were further purified by Benzamidine column chromatography (Figure 1B, lane 4), Q-Sepharose column chromatography (Figure 1B, lane 5) and SP-Sepharose column chromatography (Figure 1B, lane 6). About 10 mg of purified $RAD54B_{26–225}$ were obtained from 2.5 l of *E. coli* suspension culture. The SDS–PAGE analysis of the final purification fraction revealed an additional band with an apparent molecular weight of about 50 kDa. The band disappeared when higher concentrations of reducing agent were included in the electrophoresis sample buffer, indicating that $RAD54B_{26–225}$ oligomerizes. Consistent with this observation, a gel filtration analysis of the purified $RAD54B_{26–225}$ indicated that the fragment primarily exists as a dimer (Figure 1C). These results demonstrated that amino acid residues 26–225 of RAD54B form a stable domain. Although it is not known whether the full-length RAD54B protein multimerizes, the N-terminal region may play a role in the self-association of RAD54B.

DNA-binding activity of $RAD54B_{26–225}$

The conserved region of RAD54B (amino acid residues 321–785) contains the helicase motifs involved in DNA binding. As expected, the full-length RAD54B has both

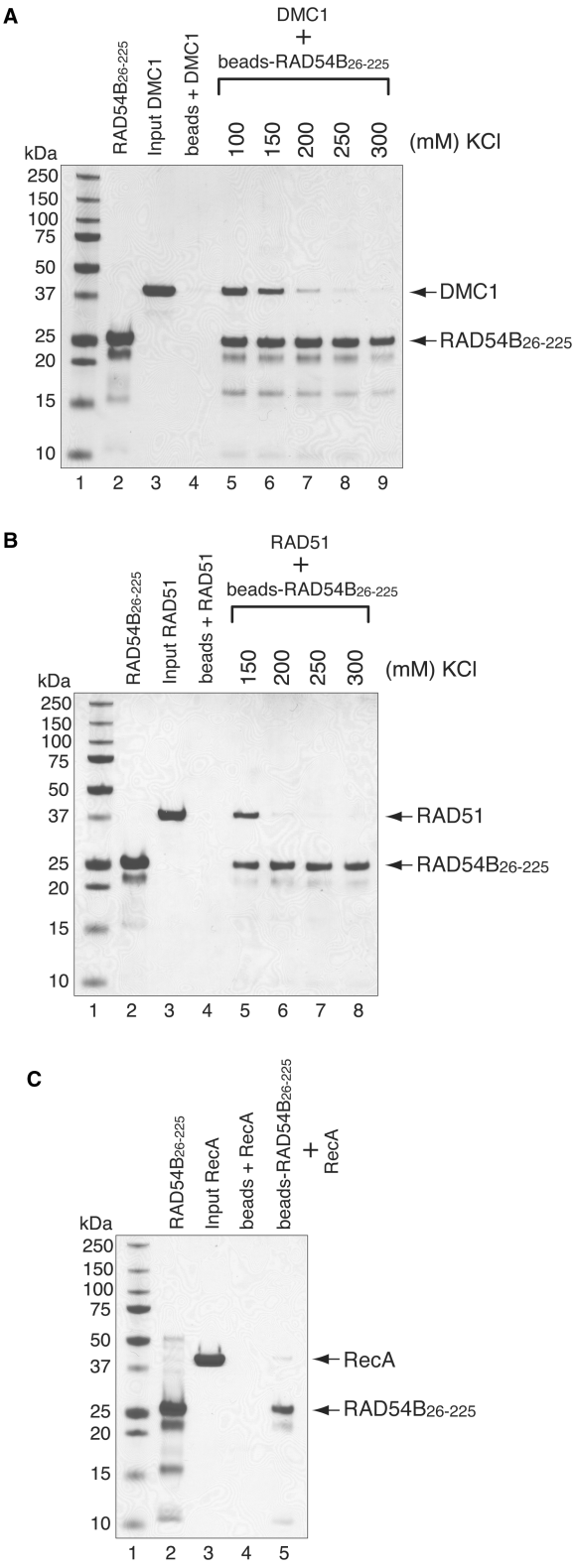

Figure 3. $RAD54B_{26–225}$ interacts with RAD51 and DMC1. The interactions were observed by a pull-down assay, in which DMC1 (**A**) or RAD51 (**B**) was mixed with $RAD54B_{26–225}$ that was covalently conjugated to an Affi-Gel 15 matrix. The proteins bound to the $RAD54B_{26–225}$-conjugated beads were eluted by SDS–PAGE sample buffer, and fractionated on a 12% SDS–PAGE gel. Lanes 2 and 3 are one-tenth of the total proteins used. Lane 4 is the negative control using the Affi-Gel 15 matrix without $RAD54B_{26–225}$. The salt concentration was titrated for both binding experiments, which are shown beyond lane 5. (**C**) Interaction between bacterial RecA and $RAD54B_{26–225}$. The binding experiment was performed in the presence of 100 mM KCl. The bands were visualized by Coomassie Brilliant Blue staining.

ssDNA- and dsDNA-binding activities (28). In contrast, the less conserved N-terminal domain of RAD54B has no known DNA-binding motifs, and it is not known whether this domain binds to DNA. Therefore, we first examined the DNA-binding activity of $RAD54B_{26–225}$, using plasmid ssDNA and dsDNA substrates. As shown in Figure 2A, $RAD54B_{26–225}$ bound to both plasmid ssDNA and dsDNA. To further characterize the DNA-binding activity of $RAD54B_{26–225}$, oligonucleotide substrates were used. $RAD54B_{26–225}$ bound to a polyA ssDNA oligonucleotide, a substrate that is free of secondary structures (Figure 2B). The binding was observed at higher salt concentrations (Figure 2C), suggesting that $RAD54B_{26–225}$ interacts with ssDNA through specific interactions and not by nonspecific ionic interactions. $RAD54B_{26–225}$ also interacted with a dsDNA oligonucleotide, as well as DNA oligonucleotides with branched structures (Figure 2D). The binding experiments were performed using the same concentrations of the DNA substrates (0.2 μM) and RAD54B (2, 4, 8 and 16 μM), to facilitate comparisons between the results with different DNA substrates. We found that $RAD54B_{26–225}$ exhibited slightly higher affinity for dsDNA than ssDNA (compare the amount of uncomplexed DNA between Figure 2B, lane 5 and 2D, lane 5). This was also apparent from the higher affinity for dsDNA than for DNA substrates with shorter duplex regions, such as the splayed arm and the 3′-tailed or 5′-tailed duplexes (Figure 2D, lanes 1–20). We also found that among the branched DNA substrates we tested, $RAD54B_{26–225}$ displayed the highest affinity for 5′-flapped DNA and 3′-PX junction (Figure 2D, lanes 26–35). These results suggested that $RAD54B_{26–225}$ may specifically function on branched DNA molecules.

$RAD54B_{26–225}$ interacts with both RAD51 and DMC1

We have previously shown that RAD54B interacts with RAD51 and DMC1 (30). However, it is not known whether the N-terminal domain of RAD54B is involved in the interactions. We therefore tested the interactions between the N-terminal domain of RAD54B and RAD51 or DMC1 by a pull-down assay, using $RAD54B_{26–225}$-conjugated Affi-Gel 15 beads. The proteins bound to the $RAD54B_{26–225}$ beads were detected by SDS–PAGE. Consistent with the fact that $RAD54B_{26–225}$ self-associates (Figure 1C), we observed $RAD54B_{26–225}$ in the elution fraction that was not covalently conjugated to the Affi-Gel beads (Figure 3A, lanes 5–9; 3B, lanes 5–8 and 3C, lane 5). As shown in Figures 3A and B, $RAD54B_{26–225}$ interacted with both RAD51 and DMC1 (Figure 3A, lanes 5–9 and 3B, lanes 5 and 6, respectively). In contrast, $RAD54B_{26–225}$ weakly bound to RecA, the bacterial homolog of RAD51 and DMC1, suggesting that the interactions between $RAD54B_{26–225}$ and RAD51 or DMC1 were specific (Figure 3C). When the salt concentrations

were titrated for the RAD51- and DMC1-binding experiments, the amounts of RAD51 and DMC1 bound to $RAD54B_{26–225}$ sharply decreased at 200 mM of KCl (Figure 3A, lane 7 and 3B, lane 6). In the case of DMC1, the binding was observed even at 300 mM of KCl, whereas the RAD51 binding was absent at 250 mM of KCl. This difference in binding affinities could reflect the differences in the mechanisms of interactions between $RAD54B_{26–225}$ and RAD51 or DMC1.

Interaction of $RAD54B_{26–225}$ with ssDNA- and dsDNA-bound DMC1

We next addressed whether $RAD54B_{26–225}$ can interact with the DMC1 protein bound to either ssDNA or dsDNA. To do this, DMC1–DNA complexes were initially formed, followed by the addition of $RAD54B_{26–225}$ and the resulting complexes were examined by a gel shift assay. To minimize the chance of $RAD54B_{26–225}$ binding to the DMC1-free regions of the DNA molecule, we determined the concentrations of DMC1 required to nearly saturate the DNA substrates (Figure 4A, lanes 4 and 9). These concentrations of DMC1 were incubated with ssDNA or dsDNA, followed by the addition of $RAD54B_{26–225}$ to the reaction mixture. As shown in Figure 4B (lanes 3–6 and lanes 10–13), increasing concentrations of $RAD54B_{26–225}$ resulted in the supershifting of the DMC1–DNA complexes in the agarose gel. The supershifted complexes migrated differently from the $RAD54B_{26–225}$–DNA complex (Figure 4B, lanes 7 and 14). These results indicated that $RAD54B_{26–225}$ can form ternary complexes with DMC1 and either ssDNA or dsDNA. In the experiments shown in Figure 4B (lanes 13 and 14), the migration distances of the DMC1–$RAD54B_{26–225}$–dsDNA ternary complex and the $RAD54B_{26–225}$–dsDNA complex were nearly the same. To exclude the possibility that DMC1 had dissociated from the DNA, leaving behind the $RAD54B_{26–225}$–dsDNA complex, we performed an electroelution of the protein–DNA complex, to investigate whether it contained DMC1. As confirmed by SDS–PAGE, both DMC1 and $RAD54B_{26–225}$ were detected (Figure 4C), indicating that the DMC1–$RAD54B_{26–225}$–dsDNA ternary complex was actually formed.

Identification of the DMC1 region that binds to $RAD54B_{26–225}$

Previously, we found that RAD54B interacts with the ATPase domain of DMC1. To define more precisely the regions of DMC1 that interact with RAD54B, 10 DMC1 fragments were designed to cover the entire region of the DMC1 sequence (Figure 5A). These fragments were expressed as GST-fused proteins. The GST-fused DMC1 fragments required a short induction time and rapid purification. Otherwise, the fragments readily degraded to a size of about 25 kDa, which is likely GST. Even with careful purification, partial degradation products were observed with some of the DMC1 fragments (Figure 5B, lanes 3, 4, 5, 7–9). A pull-down assay using GS4B beads was carried out (Figure 5B). In this assay, $RAD54B_{26–225}$ was pulled down with GST-fused DMC1 fragments

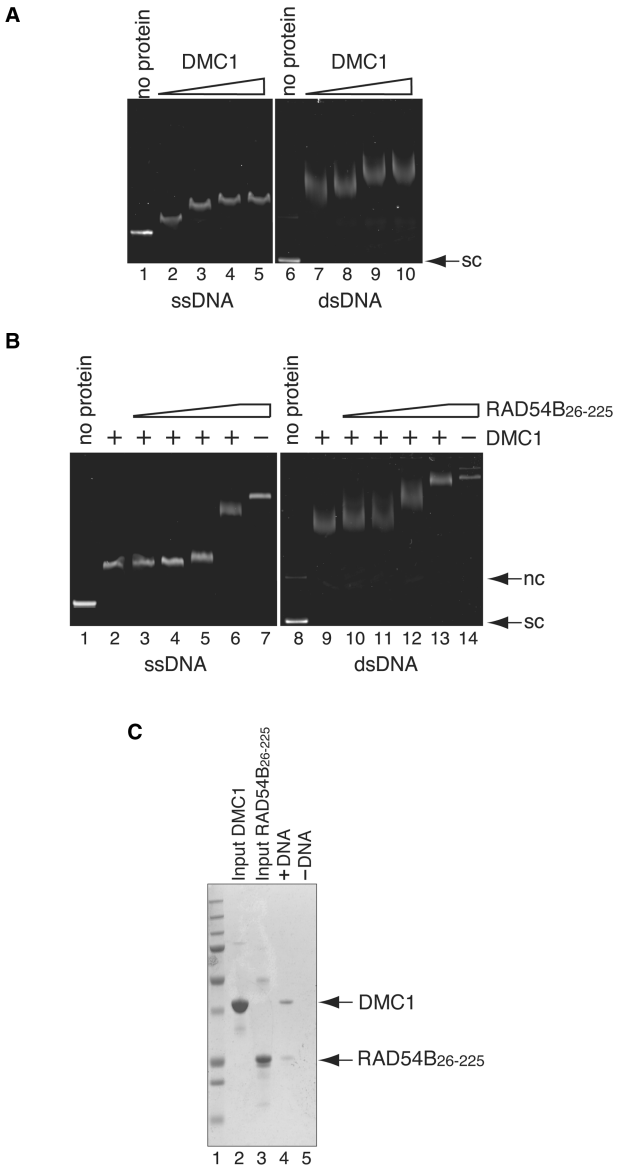

Figure 4. Interaction between DMC1 and $RAD54B_{26–225}$ on DNA. (**A**) DNA-binding activity of DMC1. Increasing amounts of DMC1 (10, 20, 40 and 80 μM in lanes 2–5 and lanes 7–10, respectively) were incubated with ϕX174 ssDNA (20 μM in nucleotides) or ϕX174 superhelical dsDNA (10 μM in nucleotides). Lanes 1 and 6 indicate negative control experiments without protein. The reaction mixtures were fractionated on a 1% agarose gel, which was stained with ethidium bromide. (**B**) $RAD54B_{26–225}$ forms ternary complexes with DMC1 and DNA. A constant amount of DMC1 (40 μM) was incubated with ϕX174 circular ssDNA (20 μM in nucleotides) or ϕX174 superhelical dsDNA (10 μM in nucleotides) at 37°C for 20min, followed by an incubation with increasing amounts of $RAD54B_{26–225}$ (0, 2.0, 4.0, 8.0 and 16 μM in lanes 2–6 and lanes 9–13, respectively) at 37°C for 20 min. In lanes 7 and 14, $RAD54B_{26–225}$ (16 μM) was incubated with ssDNA and dsDNA, but not DMC1, respectively. Lanes 1 and 8 indicate negative control experiments without protein. (**C**) Electroelution analysis of the protein–DNA complex. The protein–DNA complex detected in Figure 4B lane 13 was electroeluted from the agarose gel, and was analyzed by 12% SDS–PAGE gel (lane3). Lane 5 is the negative control experiment performed without dsDNA. Lane 1 indicates the molecular mass markers. *Lanes 2 and 3* are one-tenth of the input DMC1 and $RAD54B_{26–225}$, respectively. Nc and sc indicate nicked circular and superhelical dsDNA, respectively.

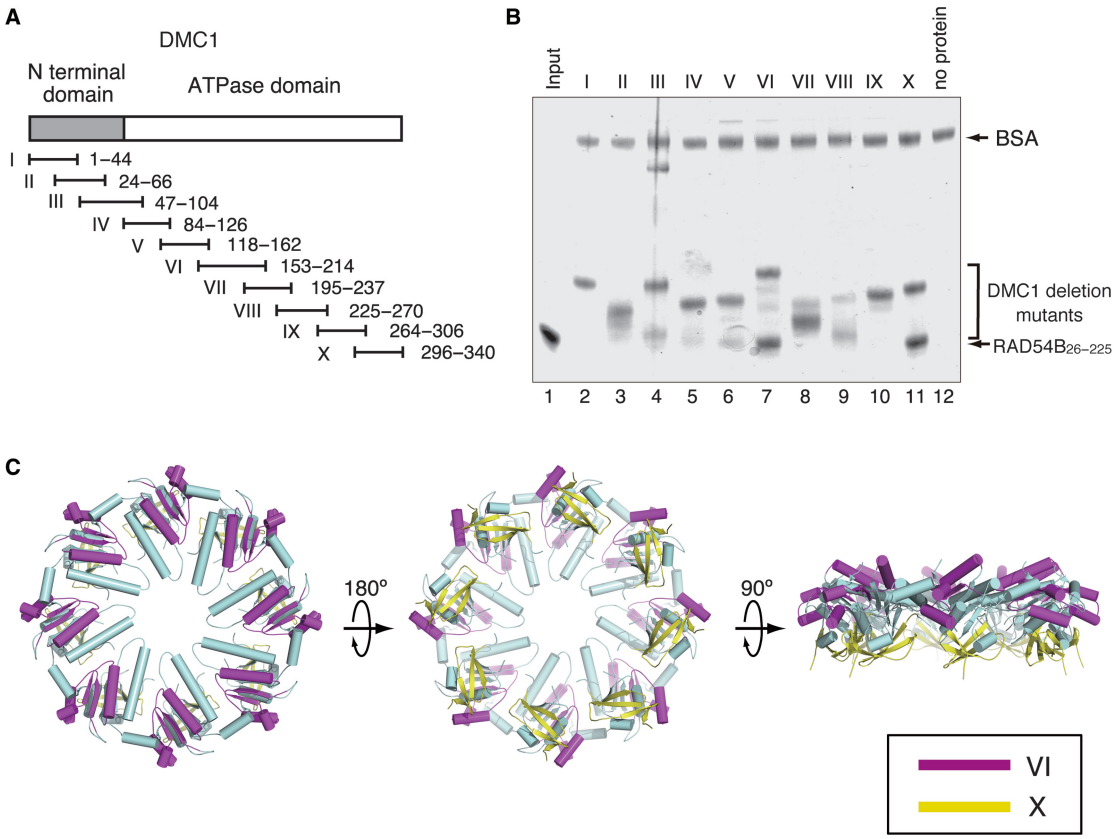

Figure 5. (**A**) A schematic representation of the 10 overlapping GST–DMC1 fusion proteins. The gray bar indicates the N-terminal domain of DMC1, and the white bar indicates the core ATPase domain. (**B**) Protein–protein interaction assay of $RAD54B_{26–225}$ with the DMC1 deletion mutants. The GS4B–DMC1 deletion mutant beads were first mixed with BSA, to prevent nonspecific protein binding, followed by the addition of $RAD54B_{26–225}$. After an incubation at 4°C for 1 h, the GS4B–DMC1 deletion mutant beads were washed with binding buffer. The $RAD54B_{26–225}$ proteins that bound to the GS4B–DMC1 deletion mutant beads were fractionated by 12% SDS–PAGE gel (lanes 2–11, respectively). Lane 1 is one-tenth of the input proteins, and lane 12 is the negative control experiment using the GS4B beads without the DMC1 deletion mutant. (**C**) The $RAD54B_{26–225}$-binding sites mapped on the DMC1 octameric ring. The purple region indicates $DMC1_{153–214}$, and the yellow region indicates $DMC1_{296–340}$.

bound to GS4B beads, and was detected by SDS–PAGE. As shown in Figure 5B, $RAD54B_{26–225}$ bound to DMC1 fragments VI and X, and weakly to V (Figure 5B, lanes 6, 7 and 11), but did not bind to other fragments. Regions VI and X are located close to each other and are exposed on the surface of the crystal structure of DMC1 (Figure 5C). The $RAD54B_{26–225}$ bound to DMC1 fragments VI and X with relatively high affinity, and these DMC1 fragments were relatively stable, suggesting that the interactions are specific.

DISCUSSION

Several studies have indicated that RAD54B and Rad54 have similar biochemical properties (29,30,38,39). To clarify the similarities and differences between RAD54B and Rad54, we focused on the poorly characterized N-terminal region of RAD54B, which shares less conservation with the corresponding region in RAD54. We found a stable domain of RAD54B that is composed of amino acid residues 26–225. This region seems to be absent in RAD54, as no structured domains were found outside the crystal structure of the core region of the zebrafish Rad54 protein (amino acid residues 91–738; Figure 1A; see Ref. 40).

The $RAD54B_{26–225}$ fragment self-associates and exists primarily as a dimer in solution. We also found that the $RAD54B_{26–225}$ fragment has both ssDNA- and dsDNA-binding activities. Among the branched DNA substrates tested, $RAD54B_{26–225}$ exhibited the highest affinities for 5′-flapped DNA and 3′-PX junction. Interestingly, cross-linking studies of the RAD54 protein demonstrated that the fundamental unit of this protein is a dimer (41). Furthermore, the RAD54 protein preferentially binds to branched DNA substrates, with the highest preference for PX junction (42). These activities are proposed to be the basis for the specific recognition of the branched DNA substrate by oligomeric RAD54 (42). Our result suggested that RAD54B may similarly self-associate on DNA, and that the N-terminal region could provide important interactions for the oligomerization and the DNA binding.

The $RAD54B_{26–225}$ fragment also physically interacted with both the RAD51 and DMC1 recombinases. Previously, we demonstrated that RAD54B stimulates the DMC1-mediated strand exchange by stabilizing the

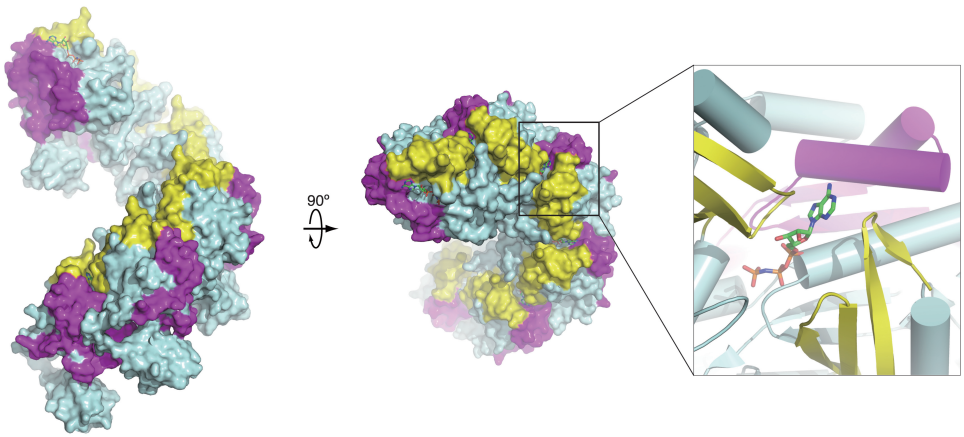

Figure 6. Proposed orientations of the RAD54B$_{26–225}$-interacting regions of DMC1 in the helical filament form. DMC1 sites essential for the interaction with RAD54B$_{26–225}$ were mapped on the corresponding locations of the *M. voltae* RadA filament. The closeup view shows the ATP-binding site that is surrounded by the RAD54B$_{26–225}$-interacting regions. All structural figures were prepared using the PyMOL program (44).

DMC1–ssDNA complex, and proposed that RAD54B may promote the formation of the active DMC1 helical filament (30). In this study, we found that RAD54B$_{26–225}$ bound to both DMC1 alone and DMC1 complexed with DNA, and we mapped the RAD54B-interacting regions of DMC1 (amino acid residues 153–214 and 296–340). These regions are exposed on the surface of the octameric ring. The corresponding regions in the *Methanococcus voltae* RadA protein, a homolog of DMC1 that forms a helical filament (43), are also exposed on the surface. Thus, the RAD54B-interacting regions appear to be easily accessible by other factors, in both the ring and helical filament forms. These regions, for example, do not overlap with the putative DNA-binding loops L1 and L2 (amino acid residues 235–240 and 271–286) that face towards the center of the ring or the filament structure. This fact is consistent with the results that RAD54B$_{26–225}$ interacted with the DMC1 bound to either ssDNA or dsDNA. Interestingly, the corresponding RAD54B-interacting regions of RadA are located near the monomer–monomer interface, and contain amino acid residues that directly interact with ATP (Figure 6). Thus, the N-terminal region of RAD54B may affect the quaternary structure of DMC1 through these interactions, and may be critical for regulating the function of DMC1. Given that RAD54B stimulates the DMC1-mediated DNA strand exchange, one possibility is that the binding of RAD54B to DMC1 may trigger the conversion of the DMC1 structure from the octameric ring form to the active helical filament form. Another possibility is that the binding of RAD54B to DMC1 may promote the turnover of DMC1 from the DNA strand-exchange product, leading to the release of DMC1. Although these observations suggested that the interaction between RAD54B and DMC1 is functionally important, meiosis in the *RAD54B* knockout mouse seems to be unaffected (29). This may be due to the presence of an unidentified RAD54 paralog that functions in meiosis. Alternatively, RAD54B may have a relatively minor role in meiosis, and may function with DMC1 only under certain circumstances. Further *in vivo* and *in vitro* analyses are required to elucidate the role of RAD54B in meiosis.

In conclusion, the present study demonstrated that the N-terminal region of RAD54B is multifunctional. We found several novel biochemical properties of the N-terminal region of RAD54B that were not previously shown for the corresponding region in RAD54. These activities may be essential for the specialized role of RAD54B in homologous recombination. More studies are required to understand the broad functional spectra of RAD54B in homologous recombination, including those that are unique to RAD54B and those that are commonly shared among RAD54 paralogs.

ACKNOWLEDGEMENTS

We thank Dr Takashi Kinebuchi (Olympus) for technical assistance.

FUNDING

Targeted Proteins Research Program (TPRP); RIKEN Structural Genomics/Proteomics Initiative (RSGI) of the National Project on Protein Structural and Functional Analyses, MEXT. The Open Access publication charges for this manuscript were waived by Oxford University Press.

Conflict of interest statement. None declared.

REFERENCES

1. Cox,M.M., Goodman,M.F., Kreuzer,K.N., Sherratt,D.J., Sandler,S.J. and Marians,K.J. (2000) The importance of repairing stalled replication forks. *Nature*, **404**, 37–41.
2. Ward,J.F. (1994) The complexity of DNA damage: relevance to biological consequences. *Int. J. Radiat. Biol.*, **66**, 427–432.
3. Caldecott,K.W. (2001) Mammalian DNA single-strand break repair: an X-ra(y)ted affair. *Bioessays*, **23**, 447–455.
4. Kleckner,N. (1996) Meiosis: how could it work? *Proc. Natl Acad. Sci. USA*, **93**, 8167–8174.
5. Roeder,G.S. (1997) Meiotic chromosomes: it takes two tango. *Genes Dev.*, **11**, 2600–2621.

6. Keeney,S., Gitoux,C.N. and Kleckner,N. (1997) Meiosis-specific DNA double-strand breaks are catalyzed by Spo11, a member of a widely conserved protein family. *Cell*, **88**, 375–384.
7. Symington,L.S. (2002) Role of RAD52 epistasis group genes in homologous recombination and double-strand break repair. *Microbiol. Mol. Biol. Rev.*, **66**, 630–670.
8. Krogh,B.O. and Symington,L.S. (2004) Recombination protein in yeast. *Annu. Rev. Genet.*, **38**, 233–271.
9. Eisen,J.A., Sweder,K.S. and Hanawalt,P.C. (1995) Evolution of the SNF2 family of proteins: subfamilies with distinct sequences and functions. *Nucleic Acids Res.*, **23**, 2715–2723.
10. Swagemakers,S.M., Essers,J., de Wit,J., Hoeijmakers,J. H. and Kanaar,R. (1998) The human RAD54 recombinational DNA repair protein is a double-stranded DNA-dependent ATPase. *J. Biol. Chem.*, **273**, 28292–28297.
11. Alexiadis,V. and Kadonaga,J.T. (2002) Strand pairing by Rad54 and Rad51 is enhanced by chromatin. *Genes Dev.*, **16**, 2767–2771.
12. Alexeev,A., Mazin,A. and Kowalczykowski,S.C. (2003) Rad54 protein possesses chromatin-remodeling activity stimulated by the Rad51-ssDNA nucleoprotein filament. *Nat. Struct. Biol.*, **10**, 182–186.
13. Jaskelioff,M., Van Komen,S., Krebs,J.E., Sung,P. and Peterson,C.L. (2003) Rad54p is a chromatin remodeling enzyme required for heteroduplex DNA joint formation with chromatin. *J. Biol. Chem.*, **278**, 9212–9218.
14. Wolner,B. and Peterson,C.L. (2005) ATP-dependent and ATP-independent roles for the Rad54 chromatin remodeling enzyme during recombinational repair of a DNA double strand break. *J. Biol. Chem.*, **280**, 10855–10860.
15. Alexiadis,V., Lusser,A. and Kadonaga,J.T. (2004) A conserved N-terminal motif in Rad54 is important for chromatin remodeling and homologous strand pairing. *J. Biol. Chem.*, **279**, 27824–27829.
16. Tan,T.L.R., Kanaar,R. and Wyman,C. (2003) Rad54, a Jack of all trades in homologous recombination. *DNA Repair*, **2**, 787–794.
17. Heyer,W.D., Li,X., Rolfsmeier,M. and Zhang,X.P. (2006) Rad54: the Swiss Army knife of homologous recombination? *Nucleic Acids Res.*, **34**, 4115–4125.
18. Jiang,H., Xie,Y., Houston,P., Stemke-Hale,K., Mortensen,U.H., Rothstein,R. and Kodadek,T. (1996) Direct association between the yeast Rad51 and Rad54 recombination proteins. *J. Biol. Chem.*, **271**, 33181–33186.
19. Golub,E.I., Kovalenko,O.V., Gupta,R.C., Ward,D.C. and Radding,C.M. (1997) Interaction of human recombination proteins Rad51 and Rad54. *Nucleic Acids Res.*, **25**, 4106–4110.
20. Wolner,B., van Komen,S., Sung,P. and Peterson,C.L. (2003) Recruitment of the recombinational repair machinery to a DNA double-strand break in yeast. *Mol. Cell*, **12**, 221–232.
21. Mazin,A.V., Alexeev,A.A. and Kowalczykowski,S.C. (2003) A novel function of Rad54 protein. Stabilization of the Rad51 nucleoprotein filament. *J. Biol. Chem.*, **278**, 14029–14036.
22. Petukhova,G., Stratton,S. and Sung,P. (1998) Catalysis of homologous DNA pairing by yeast Rad51 and Rad54 proteins. *Nature*, **393**, 91–94.
23. Sigurdsson,S., Van Komen,S., Petukhova,G. and Sung,P. (2002) Homologous DNA pairing by human recombination factors Rad51 and Rad54. *J. Biol. Chem.*, **277**, 42790–42794.
24. Solinger,J.A., Lutz,G., Sugiyama,T., Kowalczykowski,S.C. and Heyer,W.D. (2001) Rad54 protein stimulates heteroduplex DNA formation in the synaptic phase of DNA strand exchange via specific interactions with the presynaptic Rad51 nucleoprotein filament. *J. Mol. Biol.*, **307**, 1207–1221.
25. Bugreev,D.V., Mazina,O.M. and Mazin,A.V. (2006) Rad54 protein promotes branch migration of Holliday junction. *Nature*, **442**, 590–593.
26. Solinger,J.A., Kiianitsa,K. and Heyer,W.D. (2002) Rad54, a Swi2/Snf2-like recombinational repair protein, disassembles Rad51:dsDNA filaments. *Mol. Cell*, **10**, 1175–1188.
27. Hiramoto,T., Nakanishi,T., Sumiyoshi,T., Fukuda,T., Matsuura,S., Tauchi,H., Komatsu,K., Shibasaki,Y., Inui,H., Watatani,M. *et al.* (1999) Mutation of a novel human RAD54 homologue, RAD54B, sin primary cancer. *Oncogene*, **18**, 3422–3426.
28. Tanaka,K., Kagawa,W., Kinebuchi,T., Kurumizaka,H. and Miyagawa,K. (2002) Human Rad54B is a double-stranded DNA-dependent ATPase and has biochemical properties different from its structural homolog in yeast, Tid1/Rdh54. *Nucleic Acids Res.*, **30**, 1346–1353.
29. Wesoly,J., Agarwal,S., Sigurdsson,S., Bussen,W., Van Komen,S., Qin,J., Van Steeg,H., Van Benthem,J., Wassenaar,E., Baarends,W.M. *et al.* (2006) Differential contributions of mammalian Rad54 paralogs to recombination, DNA damage repair, and meiosis. *Mol. Cell Biol.*, **26**, 976–989.
30. Sarai,N., Kagawa,W., Kinebuchi,T., Kagawa,A., Tanaka,K., Miyagawa,K., Ikawa,S., Shibata,T., Kurumizaka,H. and Yokoyama,S. (2006) Stimulation of Dmc1-mediated DNA strand exchange by the human Rad54B protein. *Nucleic Acids Res.*, **34**, 4429–4437.
31. Sehorn,M.G., Sigurdsson,S., Bussen,W., Unger,V.M. and Sung,P. (2004) Human meiotic recombinase Dmc1 promotes ATP-dependent homologous DNA strand exchange. *Nature*, **429**, 433–437.
32. Zhang,Z., Fan,H.Y., Goldman,J.A. and Kingston,R.E. (2007) Homology-driven chromatin remodeling by human RAD54. *Nat. Struct. Mol. Biol.*, **14**, 397–405.
33. Kagawa,W., Kurumizaka,H., Ikawa,S., Yokoyama,S. and Shibata,T. (2001) Homologous pairing promoted by the human Rad52 protein. *J. Biol. Chem.*, **276**, 35201–35208.
34. Kinebuchi,T., Kagawa,W., Enomoto,R., Tanaka,K., Miyagawa,K., Shibata,T., Kurumizaka,H. and Yokoyama,S. (2004) Structural basis for octameric ring formation and DNA interaction of the human homologous-pairing protein Dmc1. *Mol. Cell*, **14**, 363–374.
35. Parsons,C.A., Kemper,B. and West,S.C. (1990) Interaction of a four-way junction in DNA with T4 endonuclease VII. *J. Biol. Chem.*, **265**, 9285–9289.
36. Whitby,M.C. and Dixon,J. (1998) Targeting Holliday junctions by the RecG branch migration protein of Escherichia coli. *J. Biol. Chem.*, **273**, 35063–35073.
37. Osman,F., Dixon,J., Doe,C.L. and Whitby,M.C. (2003) Generating crossovers by resolution of nicked Holliday junctions: a role for Mus81-Eme1 in meiosis. *Mol. Cell*, **12**, 761–774.
38. Miyagawa,K., Tsuruga,T., Kinomura,A., Usui,K., Katsura,M., Tashiro,S., Mishima,H. and Tanaka,K. (2002) A role for RAD54B in homologous recombination in human cells. *EMBO J.*, **21**, 175–180.
39. Tanaka,K., Hiramoto,T., Fukuda,T. and Miyagawa,K. (2000) A novel human rad54 homologue, Rad54B, associates with Rad51. *J. Biol. Chem.*, **275**, 26316–26321.
40. Thoma,N.H., Czyzewski,B.K., Alexeev,A.A., Mazin,A.V., Kowalczykowski,S.C. and Pavletich,N.P. (2005) Structure of the SWI2/SNF2 chromatin-remodeling domain of eukaryotic Rad54. *Nat. Struct. Mol. Biol.*, **12**, 350–356.
41. Petukhova,G., Van Komen,S., Vergano,S., Klein,H. and Sung,P. (1999) Yeast Rad54 promotes Rad51-dependent homologous DNA pairing via ATP hydrolysis-driven change in DNA double helix conformation. *J. Biol. Chem.*, **274**, 29453–29462.
42. Mazina,O.M., Rossi,M.J., Thoma,N.H. and Mazin,A.V. (2007) Interactions of human Rad54 protein with branched DNA molecules. *J. Biol. Chem.*, **282**, 21068–21080.
43. Wu,Y., Qian,X., He,Y., Moya,I.A. and Luo,Y. (2005) Crystal structure of an ATPase-active form of Rad51 homolog from Methanococcus voltae. *J. Biol. Chem.*, **280**, 722–728.
44. DeLano,W.L. (2002) *The PyMOL Molecular Graphics System*. DeLano Scientific, San Carlos, CA, USA.